Journal of Hazardous Materials 186 (2011) 1726–1732

Contents lists available at ScienceDirect

Journal of Hazardous Materials

journal homepage: www.elsevier.com/locate/jhazmat

Liquid phase hydrodechlorination of chlorophenols at lower temperature on a novel Pd catalyst

Zhonghao Jin[a,b], Chao Yu[c], Xingyi Wang[a,*], Ying Wan[c], Dao Li[a], Guanzhong Lu[a]

[a] Laboratory for Advanced Materials, Research Institute of Industrial Catalysis, East China University of Science and Technology, Shanghai 200237, China
[b] Shanghai Research Institute of Petrochemical Technology SINOPEC, 1658 Pudong Beilu, Shanghai 201208, China
[c] Department of Chemistry, Shanghai Normal University, Shanghai 200234, China

ARTICLE INFO

Article history:
Received 21 October 2010
Received in revised form
13 December 2010
Accepted 14 December 2010
Available online 21 December 2010

Keywords:
Hydrodechlorination
Pd catalyst
Triethylamine
Chlorophenol
Mesoporous silica–carbon
nano-composites

ABSTRACT

Pd catalyst supported on mesoporous silica–carbon nano-composite (Pd/MSCN) was prepared by the method of wet impregnation, and its activity for hydrodechlorination (HDC) of 2-chlorophenol, 4-chlorophenol and 2,4-dichlorophenol was evaluated at 258–313 K under ordinary hydrogen pressure by using triethylamine (Et_3N) as a base additive. XRD analysis indicates that Pd/MSCN catalyst possesses the ordered mesostructure. Meanwhile, the results from TEM and H_2 chemisorption analysis indicate the high dispersion of Pd on MSCN with Pd nanoparticles whose average size is 3.2 nm. For the first time, the high activity of nano-size Pd on MSCN for HDC of chlorophenols was observed at 258 K. In addition, it was found that the inhibition effect of Et_3N on HDC existed obviously, and can be efficiently reduced by stepwise addition of Et_3N. The correlations of the dielectric constants of base and the polarity of solvent to the activity of Pd/MSCN for HDC of chlorophenols were obtained.

1. Introduction

Aryl chlorides are hazardous pollutants that are considered among the most harmful organic contaminants due to their acute toxicity and high bioaccumulation potential. With the ever increasing concern for environmental protection and human health, the safe disposal of aryl chloride pollutants has acquired more attention in research activities [1,2]. One of the generally adopted approaches is thermal and/or chemical oxidation, but aryl chlorides are difficult to decompose completely to CO_2, H_2O, and HCl, and the reactions are often accompanied by the formation of other toxic chlorinated chemicals such as dioxins, phosgene, and chlorine [3]. Among the various detoxification techniques available, catalytic hydrodechlorination (HDC) represents an interesting technology that can be employed under mild conditions for the treatment of both concentrated and diluted effluents. Although HDC does not result in the complete destruction of the pollutants, it is, however, a convenient means by which the chlorinated wastes can be reduced dramatically to more biodegradable effluents.

Supported Pd catalysts are receiving more and more attention for their catalytic activity in treatment of wastewaters containing chlorinated organic pollutants, especially in the HDC reactions [4–7]. High activity of Pd catalysts for the HDC of chlorinated aromatics was observed mostly at ordinary temperature [8,9]. However, the HDC over Pd catalysts at much lower temperature has so far seldom been reported. The liquid phase HDC of 2,4-dichlorophenol (2,4-DCP) on Pd/C and Pd/Al_2O_3 was investigated at 273 K [10]. Limited by the frozen point, the HDC in aqueous solution below 273 K was not feasible. In organic solutions, 10 wt.% Pd/C showed almost no activity in the HDC of 4-chlorobiphenyl at 253 K [11].

Mesoporous silica–carbon nano-composite (MSCN) is a type of potentially useful material used as support to prepare high performance heterogeneous catalysts, because of its unique properties such as well-controlled pore structures, high surface area, large and tunable pore sizes facilitating the diffusion of reactant and product inside the pores, which are unachievable in other traditional materials [12,13]. Recently, MSCN has been used as support material of metal catalyst for water-mediated coupling reactions of chlorobenzene without presence of any other phase-transfer catalysts [14]. MSCN supported metal nanoparticles whose average particle size is 3 nm presented higher activity than other catalysts reported in literatures. This may offer us an opportunity to search a novel Pd catalyst with high performance for HDC of chlorinated aromatics at lower temperature.

* Corresponding author at: P.O. 396, East China University of Science and Technology, 130 Meilonglu, Shanghai 200237, China. Tel.: +86 21 64253372; fax: +86 21 64253372.
E-mail address: wangxy@ecust.edu.cn (X. Wang).

0304-3894/$ – see front matter © 2011 Published by Elsevier B.V.
doi:10.1016/j.jhazmat.2010.12.058

The nitrogen-containing base is often used as a promoter in the HDC of various aromatic chlorides on Pd catalysts. Hara et al. reported a Pd-hydroxyapatite-catalyzed HDC of aryl chlorides in the presence of triethylamine (Et_3N) [15]. Monguchi et al. reported that Et_3N facilitates the catalytic HDC of a variety of aromatic chlorides at room temperature and under ambient hydrogen pressure [11]. However, the effect of Et_3N on the HDC at low temperature has been not investigated in details. In this work, Pd/MSCN was prepared by the method of wet impregnation, and its activity for the HDC of 2-chlorophenol (2-CP), 4-chlorophenol (4-CP) and 2,4-DCP was evaluated at 258–313 K under ordinary hydrogen pressure by using Et_3N as a base additive. The effect of Et_3N on the HDC at 258 K was investigated through different modes of feeding into the reaction mass of chlorophenols.

2. Experimental

2.1. Catalyst preparation

The ordered MSCN support was synthesized via a surfactant templating method by using soluble phenolic resins and tetraethyl orthosilicate (TEOS) as carbon and silica precursors and the triblock copolymer F127 as a structure-directing agent [12]. Soluble phenolic resins were prepared by the base-catalyzed polymerization of phenol and formaldehyde [16]. When the initial solution contained phenolic resin, TEOS, triblock copolymer F127, HCl (conc. 0.2 mol L^{-1}), and ethanol with the mass ratio of phenol/HCHO/TEOS/HCl/F127 = 0.61:0.39:2.08:1.0:1.6, the black powders after further carbonization at 1173 K for 4 h (MSCN) were composed of silica and carbon. MSCN was impregnated in 0.8 M H_2PdCl_4 aqueous solution for 24 h at 298 K, dried at 353 K for 8 h in a vacuum oven. The resulting dry solid was reduced under flowing H_2 (30 ml min^{-1}) at 473 K for 3 h in a tubular furnace, and finally, 5 wt.% Pd/MSCN catalyst determined by ICP was obtained. The same method was employed in the preparation of 5 wt.% Pd/AC catalyst which is used as a referenced sample compared with Pd/MSCN.

2.2. Characterization

The X-ray diffraction (XRD) measurements were taken on a Rigaku Dmax-3C diffractometer using Cu Kα radiation (40 kV, 30 mA, λ = 0.15408 nm). N_2 adsorption–desorption isotherms were measured at 77 K with a Quantachrome NOVA 4000e analyzer. The Brunauer–Emmett–Teller (BET) method was utilized to calculate the specific surface areas. By using the Barrett–Joyner–Halenda (BJH) model, the pore volumes and pore size distributions were derived from the adsorption branches of isotherms. Transmission electron microscopy (TEM) experiments were conduced using a JEM 2100 microscope operated at 200 kV. X-ray photoelectron spectroscopy (XPS) measurements were performed on a Perkin-Elmer PHI 5000CESCA system with a base pressure of 10^{-9} Torr. The Pd loading on the support was determined by inductively coupled plasma-atomic emission spectrometry (ICP-AES, Varian VISTA-MPX). H_2 chemisorption was conducted on a Quantachrome CHEMBET-3000 system by pulsing hydrogen on the supported Pd catalyst. Palladium surface areas (S_{Pd}) were calculated from H_2 chemisorption data by assuming that all palladium particles are spherical and the adsorption stoichiometry was one H atom per Pd metal atom [17]. Therefore, the Pd number exposed on surface area can be estimated from the calculation: $V_{ads} \times N_0/22.4 \times 10^{20} \times$ metal content (wt.%) (V_{ads} is the volume of H_2 chemisorbed). Pd particle size is estimated according to the formula $d = 5/\rho_{Pd}S_{Pd}$.

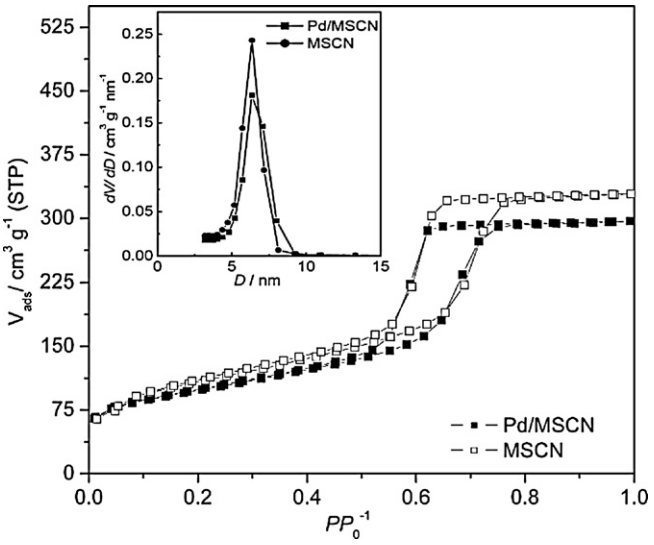

Fig. 1. Nitrogen adsorption–desorption isotherm plots and pore size distribution curves for MSCN and Pd/MSCN.

2.3. Catalytic reactions

In a typical reaction procedure, 5 wt.% Pd/MSCN (0.10 g, 47.3 μmol) was added to a stirred solution of 4-CP (0.648 g, 5 mmol), Et_3N (0.511 g, 5 mmol) and 50 ml methanol in a 100 ml three-necked flask in an iced brine bath at 258 K. The flask which contained the reaction mixture was purged 6 times with hydrogen in order to remove air completely before being stirred vigorously (1000 rpm) under ordinary hydrogen atmosphere, where Et_3N was added by one batch with 1.0 equivalence vs. the number of chlorine atoms (ENC). In the case of the stepwise addition of Et_3N, a given amount of Et_3N was added into the reaction mixture at the set-up of reaction and at given time, and the total amount of Et_3N added is 1.0 ENC. The products and reactants were analyzed by GC (Shang Fen GC112A equipped with an HP-5 column). The concentration of chloride ions in the reaction liquor was determined by using a chloride ion selective electrode. The turnover frequency (TOF) is estimated from the number of molecules transformed per surface metal atom and per second. The initial chlorophenol consumption rates were calculated from the slope of the initial portion (the conversion of reactant to isomer and hydrogenated product <10%) of plots of percent hydrogenation vs. time. In fitting the initial data the intercept of the line was forced through zero.

3. Results and discussion

3.1. Characterization

N_2 sorption isotherms of MSCN exhibit type-IV curves with a very sharp capillary condensation step at P/P_0 = 0.46–0.80 and an H_1-type hysteresis loop characterizing large-pore mesoporous materials with cylindrical channels (Fig. 1). A narrow pore size distribution with a mean value of 6.5 nm is calculated from the adsorption isotherm branch based on the BJH model. The BET surface area and pore volume of MSCN are calculated to be 413 m^2 g^{-1} and 0.53 cm^3 g^{-1}, respectively. After supporting Pd, Pd/MSCN also displays type-IV N_2 sorption isotherms with an H_1-type hysteresis loop. The capillary condensation step shifts to slightly low relative pressure range from 0.44 to 0.75, resulting from the reduction of pore size to 6.2 nm. The BET surface area and pore volume of Pd/MSCN are calculated to be 345 m^2 g^{-1} and 0.46 cm^3 g^{-1}, respectively. These phenomena can be attributed to 5 wt.% Pd inside the pores of MSCN, leading to a partial blocking of the pores.

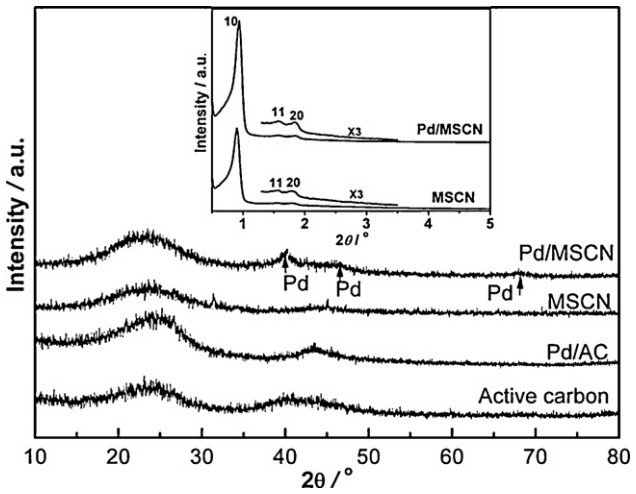

Fig. 2. Small-angle and wide-angle XRD patterns of Pd/MSCN, MSCN, Pd/AC and active carbon.

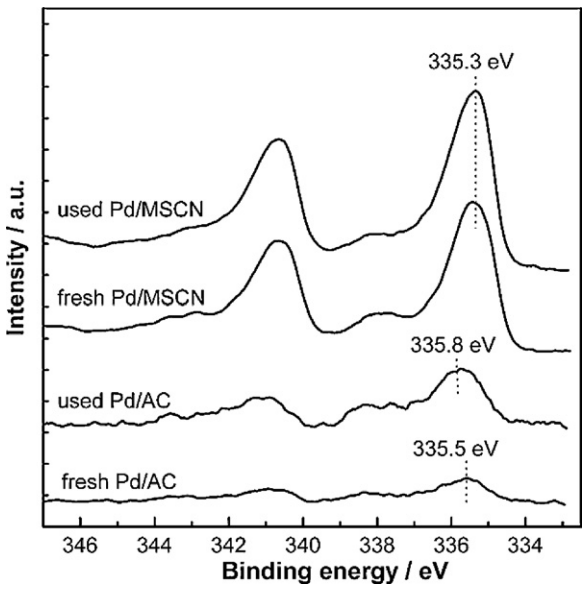

Fig. 4. XPS results of the fresh and used Pd/MSCN and Pd/AC.

MSCN and Pd/MSCN samples exhibit representative small-angle XRD patterns of the two dimensional (2-D) hexagonal mesostructure (Fig. 2), namely, one strong diffraction peak (10) at $2\theta = 0.5–1.5^\circ$ and two weak peaks (11 and 20) at higher angles. These results clearly indicate that MSCN support is stable, and the highly ordered mesostructure is retained after the impregnation of metallic solution, drying, and reduction. It should be noted that the diffraction peak intensity for Pd/MSCN is relatively weaker than that for the MSCN support. The wide-angle XRD patterns show two broad reflections at 2θ of 23 and 43°, which can be assigned to amorphous carbon. For Pd/MSCN, several peaks at 2θ of 40.1, 46.5, and 68.0° are observed, assignable to the 1 1 1, 2 0 0, and 2 2 0 reflections of the face-centered cubic (fcc) Pd lattice. It is interesting to find by TEM (Fig. 3A) that a narrow Gaussian distribution of Pd particle size is around 3.2 nm, consistent with the results obtained from H_2 titration. Compared with the Pd particle size on Pd/AC as shown in Fig. 3C, the dispersion of Pd on Pd/MSCN is much higher. The average size of Pd particles of Pd/AC is 5.1 nm as estimated from the methods mentioned above. The possible reason for the high dispersion of small-size metal particles of Pd/MSCN is the unique hybrid nature of the support. In the support, the silica and carbon components uniformly disperse on the pore wall to construct a continuous framework [12]. Pd ions may be selectively adsorbed on the surface of hydrophilic SiO_2, whose silanol groups can interact with Pd ions, while the inert, hydrophobic component carbon possibly plays a role to separate the Pd ions. XPS indicates that the intensity of Pd for Pd/MSCN is much stronger than that for Pd/AC, due to higher dispersion of Pd on Pd/MSCN and more Pd atoms to be exposed on the surface (Fig. 4). The bonding energy levels of Pd $d_{5/2}$ are 335.3 and 335.5 eV for Pd/MSCN and Pd/AC, respectively, indicating that Pd in these two catalysts acquires metal character [18]. Using the Van Hardevald and Hartog statistics, we estimated the number of different types of surface atoms on cuboctahedra Pd nanoparticles containing the same number of atoms as average nanoparticles in Pd/MSCN and Pd/AC [19]. The results show (Table S1) that the percentage of defect and face atoms with respect to the total atoms for average 3.2 nm Pd particles on Pd/MSCN are 13 and 24% respectively, while 5 and 20% for average 5.1 nm Pd particles on Pd/AC, respectively.

3.2. HDC of chlorophenols

The conversion of 4-CP on Pd/MSCN at different temperatures as a function of time is shown in Fig. 5A and TOF is listed in Table 1. At 258 K, the TOF on Pd/MSCN is $4.3 \times 10^{-2}\ s^{-1}$, greatly surpassing one on Pd/AC, $1.5 \times 10^{-2}\ s^{-1}$. It takes 600 min for the HDC of 4-CP on Pd/MSCN to complete in the presence of Et_3N (one batch addition of 1.0 ENC). This result confirms for the first time that nano-size Pd particles supported on MSCN are highly active for the

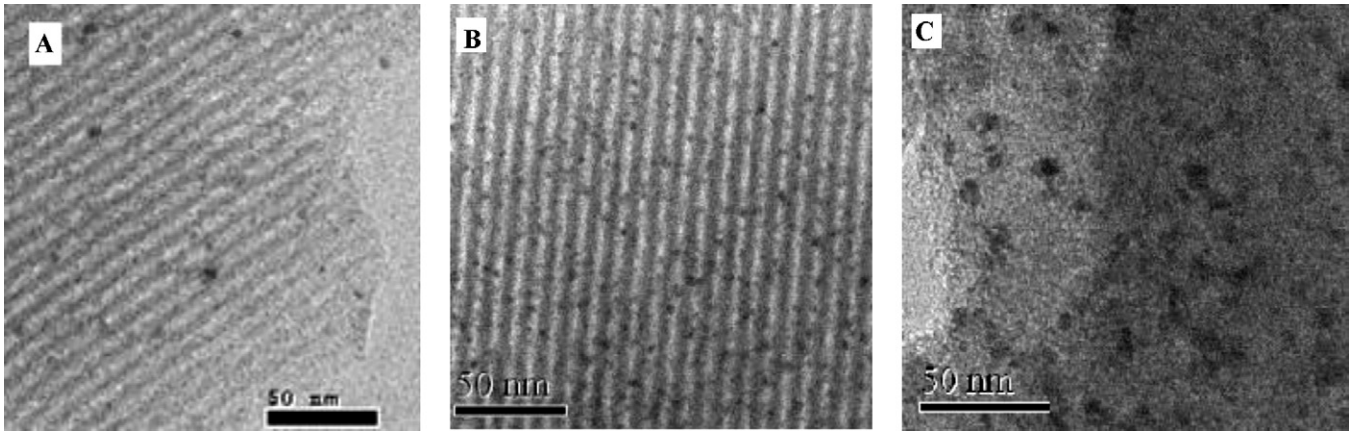

Fig. 3. TEM images of palladium catalysts: the fresh Pd/MSCN (A); the used Pd/MSCN (B); Pd/AC (C).

Table 1
Metallic size and the catalytic performance of hydrodechlorination of chlorophenols.

Sample	D_p (nm)	S_{BET} ($m^2\,g^{-1}$)	V_t ($m^3\,g^{-1}$)	d_{Pd} (nm)[a]	E_a (kJ mol^{-1})[b]	TOF × 10^2 s^{-1}				
						2-CP	4-CP			2,4-DCP
						258 K	258 K	278 K	313 K	258 K
MSCN	6.5	413	0.53							
Pd/MSCN	6.2	345	0.46	3.2	15.6(15.1)$_L$[c](15.4)$_H$	3.2(3.5)$_L$	4.3(6.1)$_L$(9.6)$_H$	4.7(7.2)$_L$(11.2)$_H$	41.7(44.2)$_L$(57.4)$_H$	5.3(5.5)$_L$
Pd/AC	3.4	727	0.21	5.1	40.8	1.3	1.5 (3.7)$_L$	3.2	36.2	1.8(4.5)$_L$

[a] Particle size, calculated from the H_2 chemisorption.
[b] Activation energy for the hydrodechlorination of 4-CP.
[c] The values within parenthesis noted with "L" obtained by stepwise addition Et_3N with amount of 0.25 ENC per 60 min; one noted with "H" obtained by stepwise addition Et_3N with amount of 0.5 ENC at 50% conversion.

HDC in liquid phase at 258 K. Phenol is the only product, and no formation of other species is observed. With raising temperature, the activity of Pd/MSCN increases obviously, as the TOF reaches $4.7 \times 10^{-2}\,s^{-1}$ at 278 K and $41.7 \times 10^{-2}\,s^{-1}$ at 313 K. Under the similar conditions, however, the activity of Pd/AC is low, and the TOF is $3.2 \times 10^{-2}\,s^{-1}$ at 278 K and $36.2 \times 10^{-2}\,s^{-1}$ at 313 K. For 2-CP, the TOF is $3.2 \times 10^{-2}\,s^{-1}$ at 258 K on Pd/MSCN, lower than that for 4-CP (Fig. 5B). This phenomenon, as reported in several literatures [20,21] comes from the steric hindrance due to the proximity of Cl substituent to hydroxyl on aromatic ring.

The activity of Pd/MSCN for the HDC of 2,4-DCP at 258 K is shown in Fig. 6. Considering the conversion of 2,4-DCP to 2-CP and 4-CP which, in turn, are converted into phenol, the corresponding TOF is estimated to be $5.3 \times 10^{-2}\,s^{-1}$ from the total number of C–Cl transformed (Table 1). Compared with the TOF for the conversion of 4-CP, the TOF for the conversion of 2,4-DCP is higher, which seems contradicted with the fact that the additional Cl substitute is deactivating [22]. This phenomenon implies that there may be some factor(s) which will affect the reaction process. The equivalence of the initial 2,4-DCP consumption rate at 258 K in formation of 2-CP (5.9 mmol g^{-1} min^{-1}) and phenol (2.7 mmol g^{-1} min^{-1}) to the HDC rate (8.6 mmol g^{-1} min^{-1}) indicates that the reaction proceeds predominantly in a stepwise fashion, converting first to 2-CP and then to phenol. Furthermore, within the total reaction time, the selectivity of 4-CP is below 1%, unlike the results obtained on Ni/SiO_2 in gas phase [20,21] at 573 K or the results obtained on Pd/AC at 258 K in liquid phase in this work, where a significant amount of 4-CP was formed (with 13% or more selectivity, Fig. S1). The TOF for 2,4-DCP on Pd/AC at 258 K is $1.8 \times 10^{-2}\,s^{-1}$ (Table 1), being much lower than one obtained on Pd/MSCN.

Doyle et al. [23] suggest that the sensitivity of catalytic hydrogenation to nanoparticle size occurs because the reaction takes place on specific types of atoms that are more (or less) prevalent on small particles. Large particles mainly contain terraces with atoms of high coordination numbers, whereas small particles contain

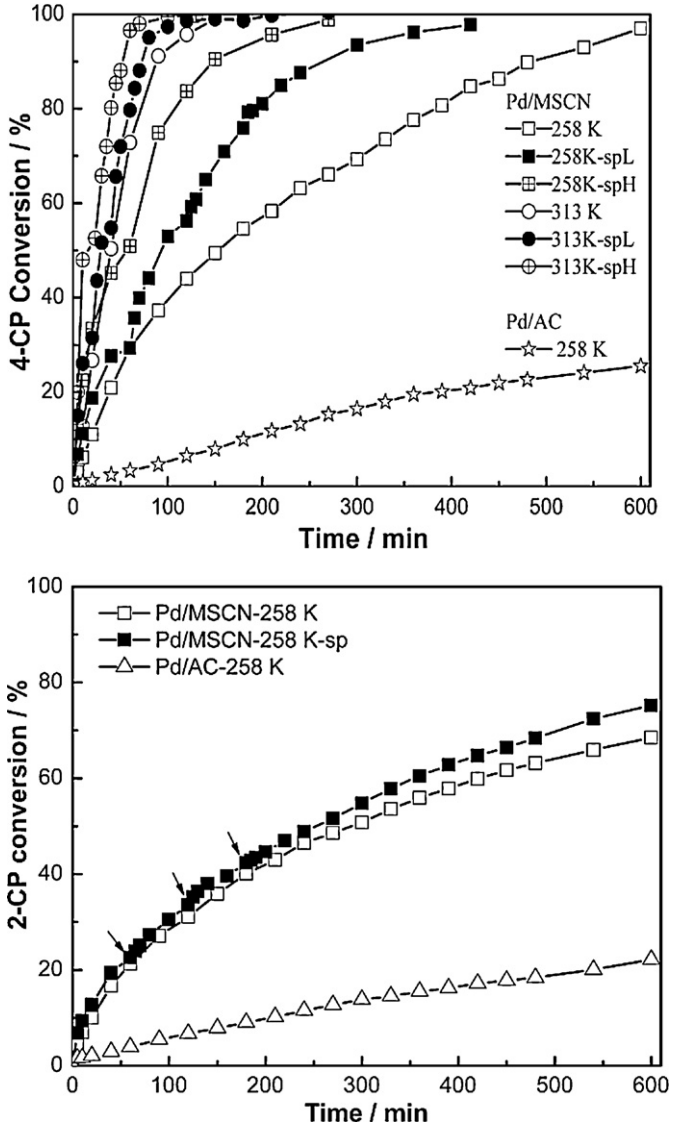

Fig. 5. HDC of 4-CP at different temperatures (A) and 2-CP at 258 K (B) over Pd/MSCN under ordinary hydrogen pressure using 1.0 ENC of Et_3N with one batch; spL: the stepwise addition of 0.25 ENC per 60 min; spH: the stepwise addition of 0. 5 ENC at 50% conversion.

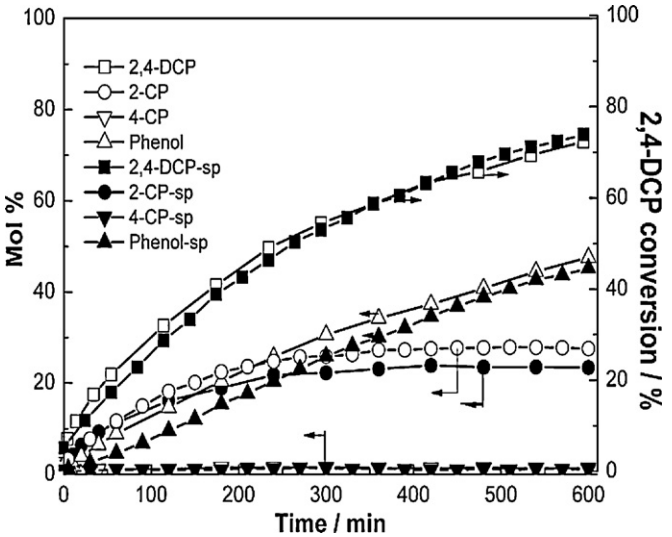

Fig. 6. HDC of 2,4-DCP over Pd/MSCN at 258 K under ordinary hydrogen pressure using 1.0 ENC of Et_3N; spL: the stepwise addition of 0.25 ENC per 60 min.

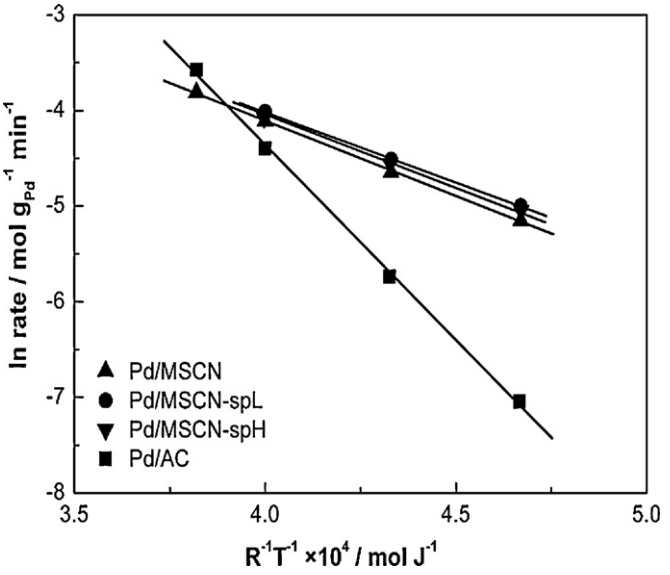

Fig. 7. Initial HDC rates for 4-CP on Pd/MSCN and Pd/AC as a function of temperature (258–313 K) under ordinary hydrogen pressure using 1.0 ENC of Et_3N with one batch; spL: the stepwise addition of 0.25 ENC per 60 min; spH: the stepwise addition of 0. 5 ENC at 50% conversion.

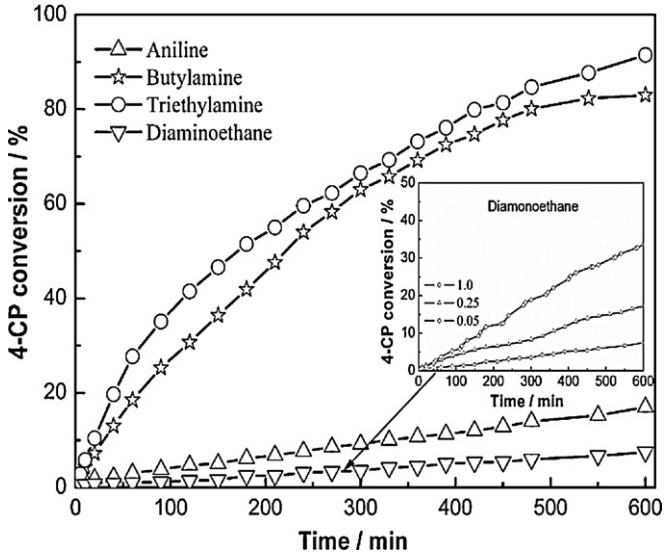

Fig. 8. The effect of different bases on the HDC of 4-CP in methanol on Pd/MSCN at 258 K; insert: the addition of DAE with 0.05 and 0.25 ENC per 60 min.

comparatively high numbers of surface atoms with low coordination numbers (edge and corner atoms). A recent study based on STM images shows that Pd nanoparticles with sizes <4 nm are highly defective, whereas nanoparticles with sizes >4 nm start to develop large and well-defined facets [24,25].

Pd nanoparticles with size of 3.2 nm on Pd/MSCN contains 13% defect atoms on the surface, on which the adsorption of 2,4-DCP may involve the coordination of the carbon–chlorine bond rather than that of the aromatic ring, The latter leads to the formation of diabsorbed aryl chloride species. In a result, both C–Cl bonds at ortho- and para-position of hydroxyl on ring would be exposed to the attack of hydrogen at the meantime and a mixture of 2-CP and 4-CP would be formed. Here, we assume the dissociative adsorption of chlorophenols via the σ-complex of C–Cl bond at 4 position (not 2 position because of the steric hindrance due to the proximity of Cl substituent to hydroxyl on aromatic ring) with the edge and corner Pd atoms on Pd/MSCN, where the aromatic ring is possibly in tilted configuration as reported [26,27], resulting in the very low selectivity of 4-CP during the HDC. Therefore, only one reaction for HDC of 2,4-DCP is possible, namely the dechlorination of the C–Cl first at 4 position and then at 2 position. In the case of Pd/AC catalyst, the defect Pd atoms possess 5%, and the surface Pd atoms exist mainly on the terraces on which the flat adsorption of 2,4-DCP via the formation of π-complex with the aromatic ring and the coordination of C–Cl bonds seems possible. Therefore, C–Cl bonds at ortho- or para-position of hydroxyl on ring can be exposed to the reaction with hydrogen so as to form the mixture of 2-CP and 4-CP.

3.3. HDC kinetics on Pd/MSCN

Taking the solubility of H_2 having no significant change within the range of 258–313 K, the pseudo-first order for the conversion of 2-CP, 4-CP and 2,4-DCP is concluded from the experimental data (Figs. S2–S5). Therefore, the conversion of chlorophenols as a function of temperature dependence of initial reaction rate can be used to generate apparent activation energies. The plots based on Arrhenius equation are shown in Fig. 7. It can be estimated from line slope that the apparent E_a value (with 95% confidence limits) of the HDC of 4-CP is 15.6 kJ mol^{-1} within this temperature range on Pd/MSCN, markedly lower than the value (40.8 kJ mol^{-1}) obtained on Pd/AC (Table 1) (as reported elsewhere [10]), and even lower than the value (24.8 kJ mol^{-1}) that has been quoted from the HDC of 4-CP promoted by Pd on carbon cloth over the temperature range 303–358 K [28]. This comparison indicates that Pd/MSCN is highly active for the HDC of chlorophenols.

3.4. The effect of base

When Et_3N is added in batches with 0.25 (per 60 min) or 0.5 (the second addition at 50% conversion) ENC, the HDC of 4-CP on Pd/MSCN is promoted greatly within the range of the Et_3N amount enough to neutralize HCl produced during HDC (Fig. 5A). In these tests, the stepwise addition of Et_3N with 0.5 ENC is more effective, and the TOF at 258 K increases up to 9.6×10^{-2} s^{-1}. Meanwhile the corresponding E_a is 15.4 kJ mol^{-1} within the range of 258–313 K (Fig. 7), almost as same as the value with one batch addition of Et_3N. This implies that the active site for the HDC of 4-CP in both cases is identical, i.e., the intrinsic activity of Pd/MSCN is not modified. The results from the interaction of Et_3N with active sites lead to the decrease in the number of the available sites for 4-CP molecules. For 2,4-DCP, however, the stepwise addition of Et_3N at 258 K affects the HDC to a small extent (Fig. 6), which implies that 2,4-DCP molecules adsorb more competitively on the active sites than Et_3N does. The different effects of Et_3N on the HDC of 4-CP and 2,4-DCP stem from the fact that Pd atoms favor to react with C–Cl of 2,4-DCP with low electron density due to the additional Cl substitution with electron withdrawing. By raising temperature to 313 K, this inhibition effect of Et_3N becomes weak. In the case of Pd/AC catalyst, the HDC of both 4-CP and 2,4-DCP is inhibited by Et_3N to a larger extent (Table 1). Therefore, the high activity for the HDC of Pd/MSCN is related to its strong interaction with chlorophenols. Without Et_3N, Pd catalysts will deactivate and the reaction rate reduces quickly, because of the strong adsorption of the formed chlorine species on the active sites.

The HDC of 4-CP over Pd/MSCN at 258 K using various bases containing N was investigated (Fig. 8). The ε of bases decreases in the order of diaminoethane > aniline > n-butylamine > Et_3N (Table 2), which matches the order of conversion increase. The ε can be influenced by the polarizability of molecules. The more polarizable the base containing nitrogen is, the more easily the pair electrons on nitrogen atom translate. In the presence of a base of high ε, such as diaminoethane, strongly coordinative to metal species, Pd/MSCN

Table 2
The HDC of 4-CP at 258 K using bases with different dielectric constants.

Base	Diaminoethane			Aniline	n-Butylamine	Triethylamine	
Dielectric constant[a]	13.8			7.1	5.4	2.4	
Addition (ENC)[b]	0.05	0.25	1.0	1.0	1.0	0.25	1.0
Initrial TOF $\times 10^2$ s^{-1}	1.48	0.75	0.33	0.70	9.50	31.0	13.7
Average TOF $\times 10^2$ s^{-1}	1.50	0.73	0.35	0.70	3.63	8.2	4.3

[a] The values at 293 K quoted from Ref. [32].
[b] 0.05 and 0.25 ENC per 60 min with total addition of 1.0 ENC.

shows a very low activity, due to the strong adsorption of base on Pd atoms. However, in the case of a base of low ε, such as Et_3N, Pd/MSCN displays much higher activity. Using the stepwise addition of diaminoethane with the amount of 0.05 and 0.25 ENC per 60 min, the TOF is increased to 1.5×10^{-2} and 0.7×10^{-2} s^{-1}, respectively, obviously higher than the value (0.33×10^{-2} s^{-1}) in the case of one batch addition. The curve of conversion vs. time (Fig. 8) is linear in the presence of diaminoethane and aniline. These phenomena indicate that the surface is saturated by these bases and the HDC is controlled by the equilibrium of base adsorption and desorption. The decrease in the concentration of bases will result in lowering the coverage of bases on Pd/MSCN, and in increasing the active sites available for 4-CP, so that TOF will increase (Fig. 8 insert).

3.5. Recycling study

For the recycling study, the HDC of 4-CP was performed under the same reaction conditions as described above. After five successive runs were tested, the TOF on used Pd/MSCN is 4.0×10^{-2} s^{-1}, similar to that on the fresh one. The Pd content of the corresponding used catalyst is 4.9 wt.%. A low Pd leaching amount (less than 0.3% of Pd content of catalyst) is detected by ICP analysis of the catalyst-free liquor. The mesostructure keeps unchanged, the dispersion of Pd particle is still high (Fig. 3B).

3.6. The effect of solvent and reaction mechanism

The HDC of 4-CP over Pd/MSCN at 258 K in the different organic solvents is shown in Fig. 9. Methanol was the most preferable solvent for this reaction, followed by acetone, i-propanol, tetrahydrofuran, ethyl ether and n-hexane. This order of activity for HDC is lined with that reported by Hara et al. [29]. The conversion profiles for all solvents could be described well by zero-order kinetics except for methanol, although the initial rates appear quite different. The observed zero-order kinetics suggests that the catalyst surface is saturated by the reacting species within the overall reaction time. Hence, 4-CP adsorption on the surface of Pd/MSCN in these five solvents must not be rate limiting. The reaction is probably limited by one of the processes on the surface that follows adsorption, e.g., reaction with hydrogen, desorption of products, or neutralization of the formed hydrogen chloride, which has an inhibition effect on the reaction [22,30,31]. In the above solvent system, a slight change of hydrogen pressure or base amount is impossible to result in a significant effect on the HDC, which implies that the desorption of products is rate limiting.

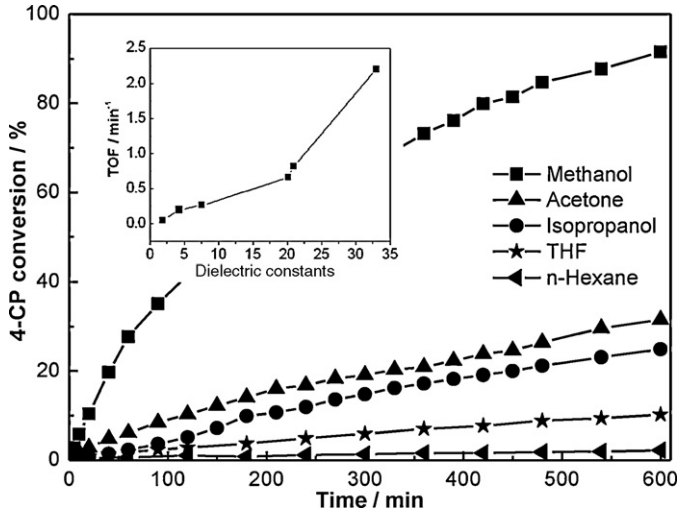

Fig. 9. HDC of 4-CP in the different solvents over Pd/MSCN at 258 K, insert: the curve of the TOF vs. the polarity of the solvent.

Two HDC routes of aromatic chlorides (ionic and free-radical) are suggested depending on the nature of the active hydrogen species [4]. If the HDC proceeds by a radical mechanism through the formation of phenyl radicals, the radicals either interact with adsorbed hydrogen atoms to form phenol or recombine to form 4,4′-biphenol. In this work, 4,4′-biphenol was not found at all, and only phenol was detected. The amount of chloride ions formed was measured to be equivalent to the amount of chlorine species contained in the chlorophenols transformed.

The dielectric constants (ε) of the solvents under study is listed in Table 2 [32]. It is interesting to find that the TOF increases with the increase in the ε of the solvents (Fig. 9 insert). As known to us, the formed chloride species will inhibit the reaction when removed slowly. The ε represents the dimension of molecule polarity. The increase in the polarity of solvent favors the transfer of chloride species from the catalyst surface to the reaction liquor through the miscibility of HCl with the polar solvent. Pd/MSCN presents the highest activity of for the HDC of 4-CP in methanol, which is related to the strong polarity of methanol.

4. Conclusion

Pd/MSCN was prepared by a wet impregnation method. XRD analysis showed that Pd/MSCN possesses the ordered mesostructure, and its BET surface area and pore diameter are calculated from N_2 adsorption isotherms to be 345 m^2 g^{-1} and 6.2 nm, respectively. A high dispersion of Pd on Pd/MSCN was observed on TEM images and the size Pd particles was estimated to be 3.2 nm from H_2 chemisorption analysis.

Pd/MSCN showed high activity for HDC of chlorophenols at 258–313K under ordinary hydrogen pressure using Et_3N as a base additive. The TOF of 2-CP, 4-CP and 2,4-DCP at 258 K is 3.2×10^{-2}, 4.3×10^{-2} and 5.3×10^{-2} s^{-1}, respectively, much higher than the values obtained on Pd/AC catalyst.

The inhibition effect of Et_3N in the HDC was observed at 258 K. The stepwise addition of Et_3N can promote the HDC of chlorophenols obviously. Additionally, it has been found that highly polar solvents and bases containing nitrogen of low ε favor the HDC of 4-CP at 258 K.

Acknowledgements

We would like to acknowledge the financial support from National Basic Research Program of China (no. 2010CB732300) and National Natural Science Foundation of China (no. 20977029).

Appendix A. Supplementary data

Supplementary data associated with this article can be found, in the online version, at doi:10.1016/j.jhazmat.2010.12.058.

References

[1] M.J. Morra, V. Borek, J. Koolpe, Transformation of Chlorinated Hydrocarbons Using Aquocobalamin or Coenzyme F430 in Combination with Zero-Valent Iron, J. Environ. Qual. 29 (2000) 706–715.
[2] F. Alonso, I.P. Beletskaya, M. Yus, Metal-mediated reductive hydrodehalogenation of organic halides, Chem. Rev. 102 (2002) 4009–4092.
[3] M.D. Erickson, S.E. Swanson, J.D. Flora Jr., G.D. Hinshaw, Polychlorinated dibenzofurans and other thermal combustion products from dielectric fluids containing polychlorinated biphenyls, Environ. Sci. Technol. 23 (1989) 462–470.
[4] T. Kawabata, I. Atake, Y. Ohishi, T. Shishido, Y. Tian, K. Takaki, K. Takehira, Liquid phase catalytic hydrodechlorination of aryl chlorides over Pd–Al-MCM-41 catalyst, Appl. Catal. B 66 (2006) 151–160.
[5] M.O. Nutt, J.B. Hughes, M.S. Wong, Designing Pd-on-Au bimetallic nanoparticle catalysts for trichloroethene hydrodechlorination, Environ. Sci. Technol. 39 (2005) 1346–1353.
[6] R. Nakao, H. Rhee, Y. Uozumi, Hydrogenation and dehalogenation under aqueous conditions with an amphiphilic-polymer-supported nanopalladium catalyst, Org. Lett. 7 (2005) 163–165.
[7] L. Calvo, M.A. Gilarranz, J.A. Casas, A.F. Mohedano, J.J. Rodríguez, Hydrodechlorination of 4-chlorophenol in aqueous phase using Pd/AC catalysts prepared with modified active carbon supports, Appl. Catal. B 67 (2006) 68–76.
[8] H. Hildebrand, K. Mackenzie, F.D. Kopinke, Highly active Pd-on-magnetite nanocatalysts for aqueous phase hydrodechlorination reactions, Environ. Sci. Technol. 43 (2009) 3254–3259.
[9] G. Yuan, M.A. Keane, Aqueous-phase hydrodechlorination of 2,4-dichlorophenol over Pd/Al_2O_3: reaction under controlled pH, Ind. Eng. Chem. Res. 46 (2007) 705–715.
[10] G. Yuan, M.A. Keane, Liquid phase catalytic hydrodechlorination of chlorophenols at 273 K, Catal. Commun. 4 (2003) 195–201.
[11] Y. Monguchi, A. Kume, K. Hattori, T. Maegawa, H. Sajiki, Pd/C-Et_3N-mediated catalytic hydrodechlorination of aromatic chlorides under mild conditions, Tetrahedron 62 (2006) 7926–7933.
[12] R.L. Liu, Y.F. Shi, Y. Wan, Y. Meng, F.Q. Zhang, D. Gu, Z.X. Chen, B. Tu, D.Y. Zhao, Triconstituent Co-assembly to ordered mesostructured polymer–silica and carbon–silica nanocomposites and large-pore mesoporous carbons with high surface areas, J. Am. Chem. Soc. 128 (2006) 11652–11662.
[13] M. Choi, F. Kleitz, D.N. Liu, H.Y. Lee, W.S. Lee, R. Ahn, Ryoo, Controlled polymerization in mesoporous silica toward the design of organic–inorganic composite nanoporous materials, J. Am. Chem. Soc. 127 (2005) 1924–1932.
[14] Y. Wan, H.Y. Wang, Q.F. Zhao, M. Klingstedt, O. Terasaki, D.Y. Zhao, Ordered mesoporous Pd/silica–carbon as a highly active heterogeneous catalyst for coupling reaction of chlorobenzene in aqueous media, J. Am. Chem. Soc. 131 (2009) 4541–4550.
[15] T. Hara, K. Mori, M. Oshiba, T. Mizugaki, K. Ebitani, K. Kaneda, Highly efficient dehalogenation using hydroxyapatite-supported palladium nanocluster catalyst with molecular hydrogen, Green Chem. 6 (2004) 507–509.
[16] Y. Meng, D. Gu, F.Q. Zhang, Y.F. Shi, H.F. Yang, Z. Li, C.Z. Yu, B. Tu, D.Y. Zhao, Ordered mesoporous polymers and homologous carbon frameworks: amphiphilic surfactant templating and direct transformation, Angew. Chem. Int. Ed. 44 (2005) 7053–7059.
[17] S.Y. Wang, S.H. Moon, M.A. Vannice, The effect of SMSI (strong metal–support interaction) behavior on CO adsorption and hydrogenation on Pd catalysts: II. Kinetic behavior in the methanation reaction, J. Catal. 71 (1981) 167–174.
[18] A.C. Thomas, Photoelectron and Auger Spectroscopy, 1st ed., Plenum, New York, 1975, p. 352.
[19] R.W.J. Scott, A.K. Datye, R.M. Crooks, Bimetallic palladium–platinum dendrimer-encapsulated catalysts, J. Am. Chem. Soc. 125 (2003) 3708–3709.
[20] E.J. Shin, M.A. Keane, Detoxification of dichlorophenols by catalytic hydrodechlorination using a nickel/silica catalyst, Chem. Eng. Sci. 54 (1999) 1109–1120.
[21] E.J. Shin, M.A. Keane, Gas phase catalytic hydrodechlorination of chlorophenols using a supported nickel catalyst, Appl. Catal. B 18 (1998) 241–250.
[22] J.B. Hoke, G.A. Gramiccioni, E.N. Balko, Catalytic hydrodechlorination of chlorophenols, Appl. Catal. B 1 (1992) 285–296.
[23] A.M. Doyle, S.K. Shaikhutdinov, H.J. Freund, Surface-bonded precursor determines particle size effects for alkene hydrogenation on palladium, Angew. Chem. Int. Ed. 44 (2005) 629–631.
[24] H.J. Freund, M. Baumer, J. Libuda, T. Risse, G. Rupprechter, S. Shaikhutdinov, Preparation and characterization of model catalysts: from ultrahigh vacuum to in situ conditions at the atomic dimension, J. Catal. 216 (2003) 223–225.
[25] J. Silvestre-Albero, G. Rupprechter, H.J. Freund, Atmospheric pressure studies of selective 1,3-butadiene hydrogenation on well-defined $Pd/Al_2O_3/NiAl(1\,1\,0)$ model catalysts: effect of Pd particle size, J. Catal. 240 (2006) 58–65.
[26] M.A. Keane, D.Yu. Murzin, A kinetic treatment of the gas phase hydrodechlorination of chlorobenzene over nickel/silica: beyond conventional kinetics, Chem. Eng. Sci. 56 (2001) 3185–3195.
[27] T. Yoneda, T. Takido, K. Konum, Hydrodechlorination of para-substituted chlorobenzenes over a ruthenium/carbon catalyst, Appl. Catal. B 84 (2008) 667–677.
[28] Y. Shindler, Y. Matatov-Meytal, M. Sheintuch, Wet hydrodechlorination of p-chlorophenol using Pd supported on an activated carbon cloth, Ind. Eng. Chem. Res. 40 (2001) 3301–3308.
[29] T. Hara, T. Kaneta, K. Mori, T. Mitsudome, T. Mizugaki, K. Ebitani, K. Kaneda, Magnetically recoverable heterogeneous catalyst: palladium nanocluster supported on hydroxyapatite-encapsulated γ-Fe_2O_3 nanocrystallites for highly efficient dehalogenation with molecular hydrogen, Green Chem. 9 (2007) 1246–1251.
[30] C.D. Thompson, R.M. Rioux, M. Chen, F.H. Ribeiro, Turnover Rate, Reaction order, and elementary steps for the hydrodechlorination of chlorofluorocarbon compounds on palladium catalysts, J. Phys. Chem. B 104 (2000) 3067–3077.
[31] M.A. Aramendía, V. Borau, I.M. García, C. Jiménez, M. Lafont, A. Marinas, J.M. Marinas, F.J. Urbano, Influence of the reaction conditions and catalytic properties on the liquid-phase hydrodechlorination of chlorobenzene over palladium-supported catalysts: activity and deactivation, J. Catal. 187 (1999) 392–399.
[32] J.G. Speight, Lange's Handbook of Chemistry, 16th ed., McGraw-Hill Professional, New York, 2005, p. 2470.